



ANS Annual Meeting 2020



Rapid Analytic Determination of Dry Cask Storage Canister Internal Temperatures

Evan Palmer

Undergraduate Student Research

Department of Mechanical Engineering and
Materials Science, University of Pittsburgh

etp18@pitt.edu

Matthew Barry, Ph.D.

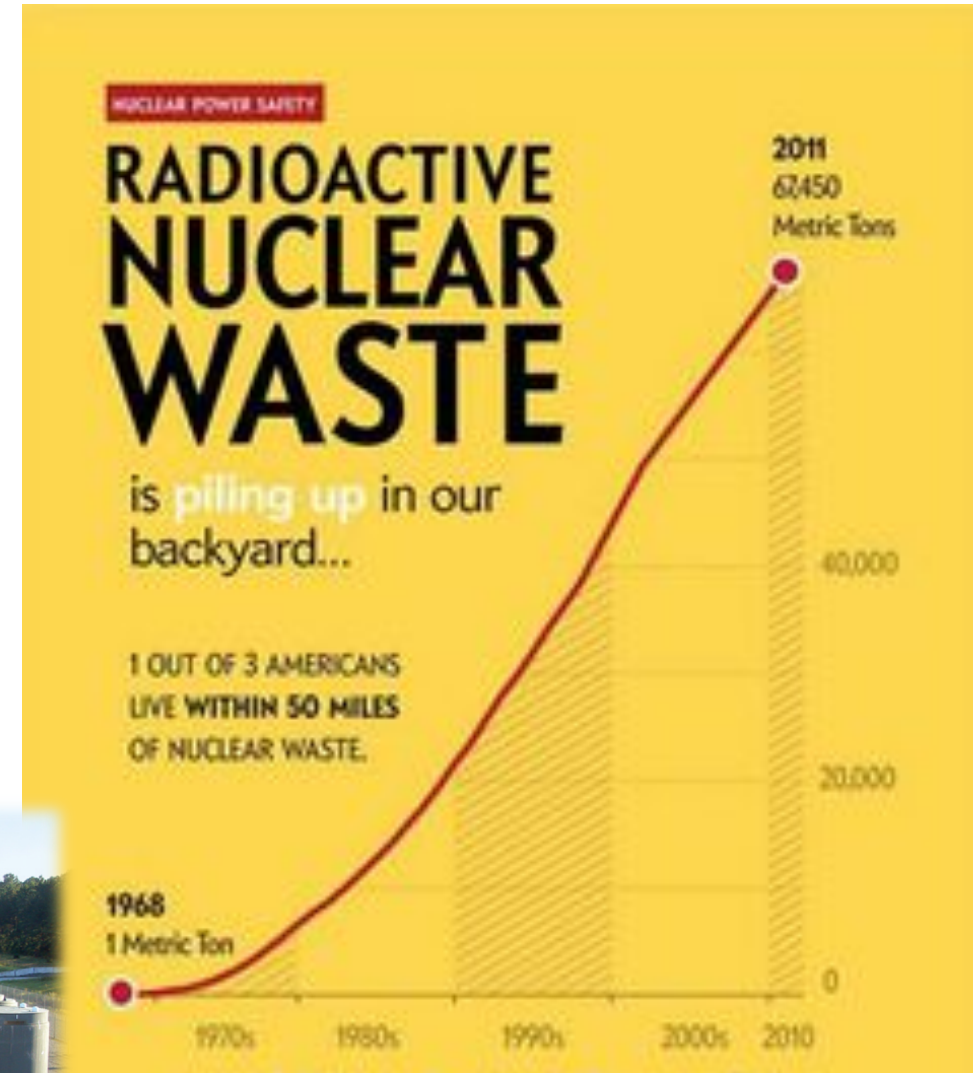
Assistant Professor

Department of Mechanical Engineering and
Materials Science, University of Pittsburgh

mmb49@pitt.edu



Dry Storage is here to stay.



Temperature is everything^[1]

Temperature Profiles

Most degradation mechanisms are temperature-dependent with rates generally increasing with temperature. Current safety analyses are appropriately based on bounding temperature profiles, but recent data has shown that high burn up cladding can become brittle at lower temperatures due to phenomena such as radial hydride precipitation. Similarly, recent models on delayed hydride cracking suggest that this mechanism may become more prolific at lower temperatures. For these reasons, the program recognizes the need to develop realistic temperature profiles for all dry storage components as a function of extended storage.

High

Calculate temperature profiles of SSCs as a function of time for representative dry cask storage systems.

USED FUEL DISPOSITION CAMPAIGN
Gap Analysis to Support Extended Storage of Used Nuclear Fuel
Rev. 0

Fuel Cycle Research & Development

Prepared for
 U.S. Department of Energy
 Used Fuel Disposition
 Campaign

Brady Hanson (PNNL)
 Halim Alsaed (INL)
 Christine Stockman (SNL)
 David Enos (SNL)
 Ryan Meyer (PNNL)
 Ken Sorenson (SNL)

January 31, 2012
 FCRD-USED-2011-000136 Rev. 0
 PNNL-20509



[1] B. HANSON, H. ALSAED, C. STOCKMAN, D. ENOS, R. MEYER, and K. SORENSEN, "Gap analysis to support extended storage of used nuclear fuel, Rev. 0," Tech. rep., Pacific Northwest National Lab.(PNNL), Richland, WA (United States); Idaho . . . (2012).

Computational Modeling^[2]:

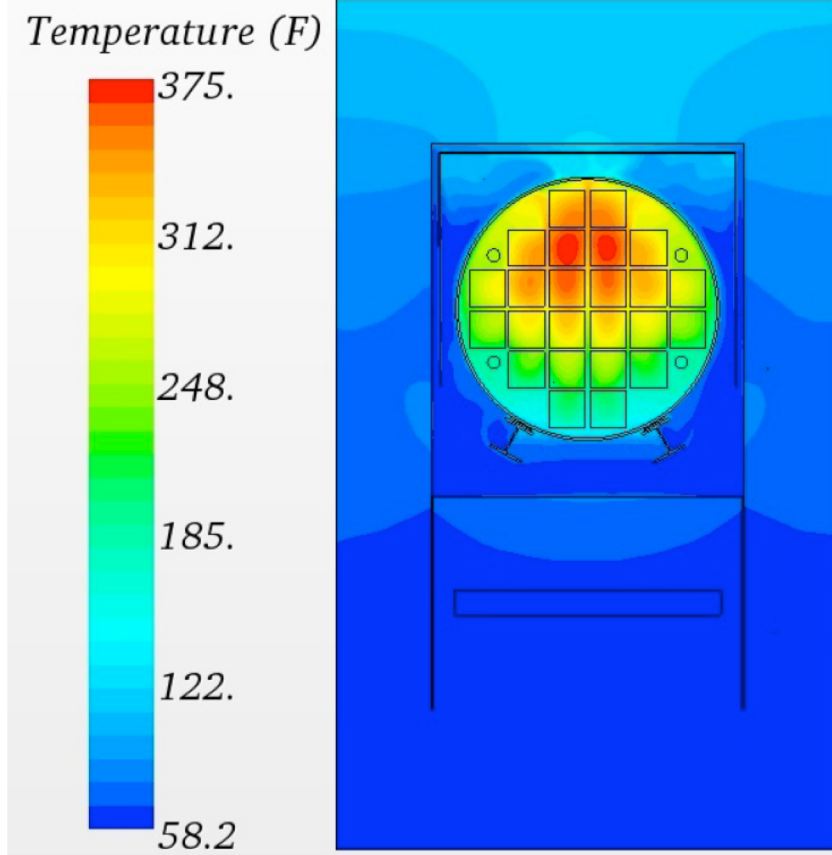


Figure 7.8. Temperature Distribution in Central Cross-section of HSM-15 for Base Case – 58°F (14°C) Ambient

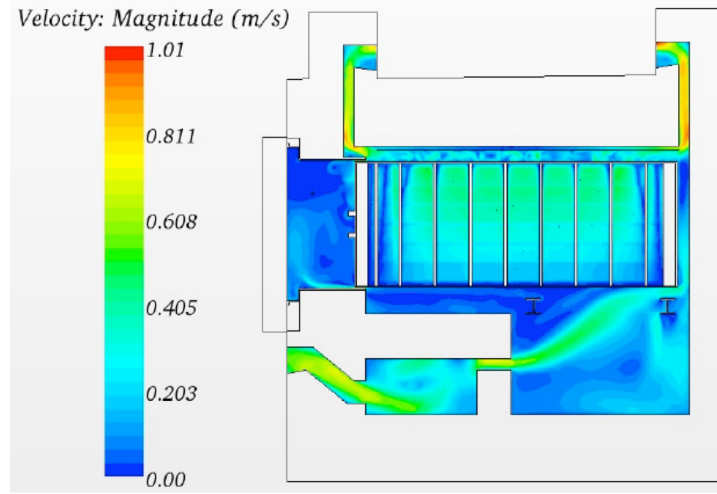


Figure S.4. Velocity at Axial Midplane for Base Case (HSM-15) – 58°F (14°C) Ambient Air

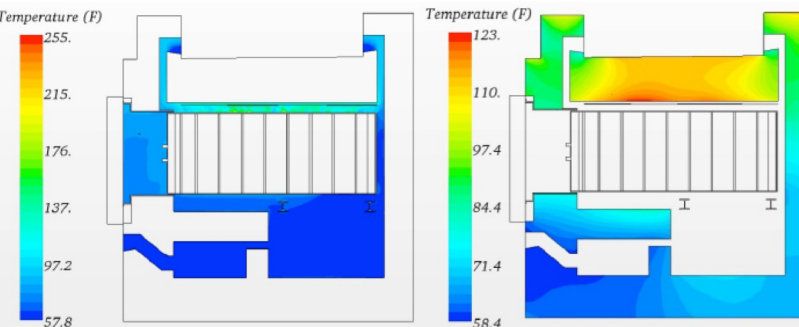


Figure S.5. Air and Concrete Temperature Distributions at Axial Midplane for Base Case (HSM-15) – 58°F (14°C) Ambient Air

PNNL-21788

U.S. DEPARTMENT OF ENERGY
Prepared for the U.S. Department of Energy under Contract DE-AC05-76RL01830

Thermal Modeling of NUHOMS HSM-15 and HSM-1 Storage Modules at Calvert Cliffs Nuclear Power Station ISFSI

SR Suffield
JA Fort
HE Adkins

JM Cuta
BA Collins
ER Siciliano

October 2012

Pacific Northwest NATIONAL LABORATORY
Proudly Operated by Battelle Since 1965



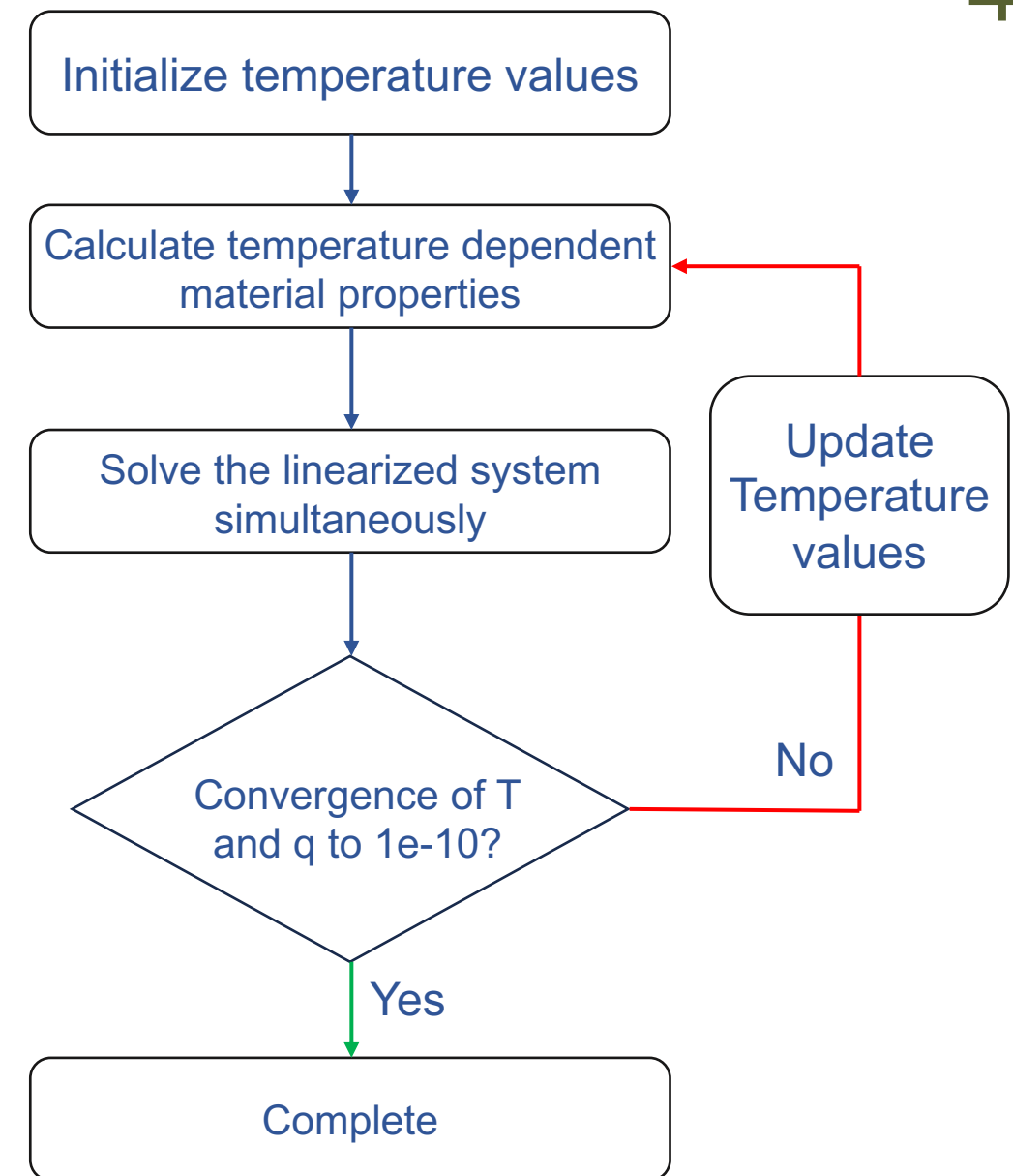
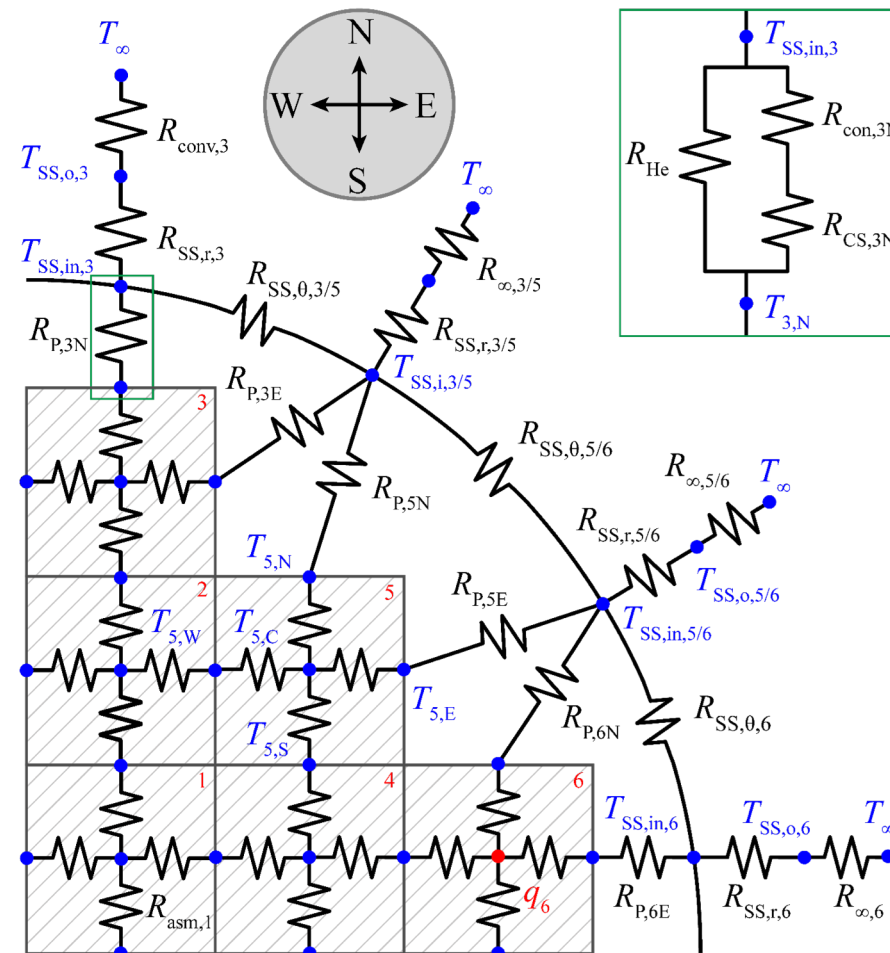
[2] S. R. SUFFIELD, J. A. FORT, H. E. ADKINS, J. M. CUTA, B. A. COLLINS, and E. R. SICILIANO, "Thermal modeling of NUHOMS HSM-15 and HSM-1 storage modules at Calvert Cliffs nuclear power station ISFSI," Tech. rep., Pacific Northwest National Lab.(PNNL), Richland, WA (United States) (2012).

Iterative Analytic Modeling:

Each component modeled using thermal resistance Network (TRN):

$$q = \frac{\Delta T}{R_{th}}$$

R_{th} includes temp-dep. thermal conductivity



Heat Transfer Considerations

- *Conduction:* Fuel Assemblies – Spacer Discs – DSC Canister
- *Convection:* Canister Surface to Ambient Air
- *Radiation:* Ignored due to relatively low temperatures, although included in [2].

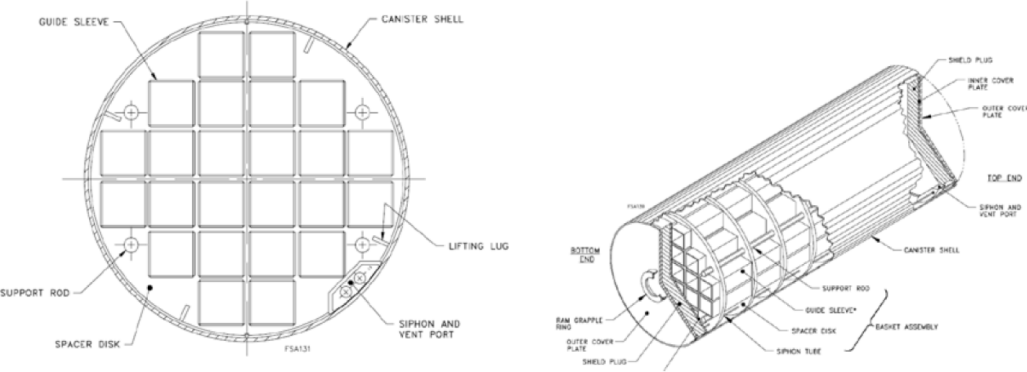


Figure 2.2. Illustrative Diagrams of 24P DSC Geometry (Images courtesy of AREVA)

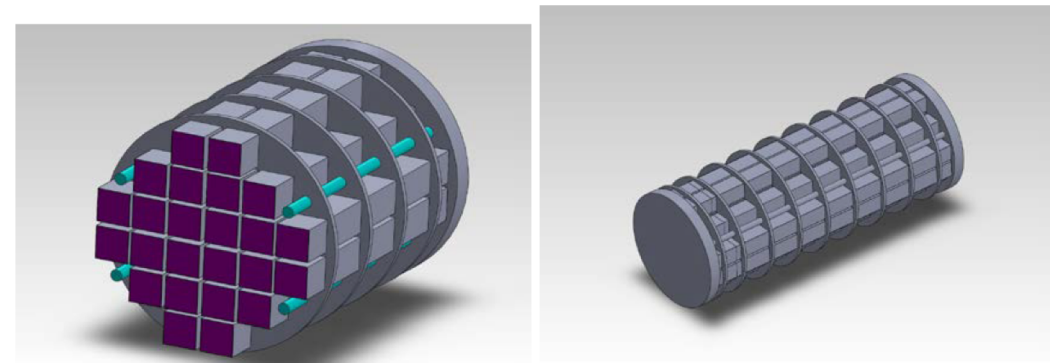


Figure 2.3. Mid-Plane Cross-Sectional View and Exterior View of Internal Geometry in SolidWorks® Model of 24P DSC



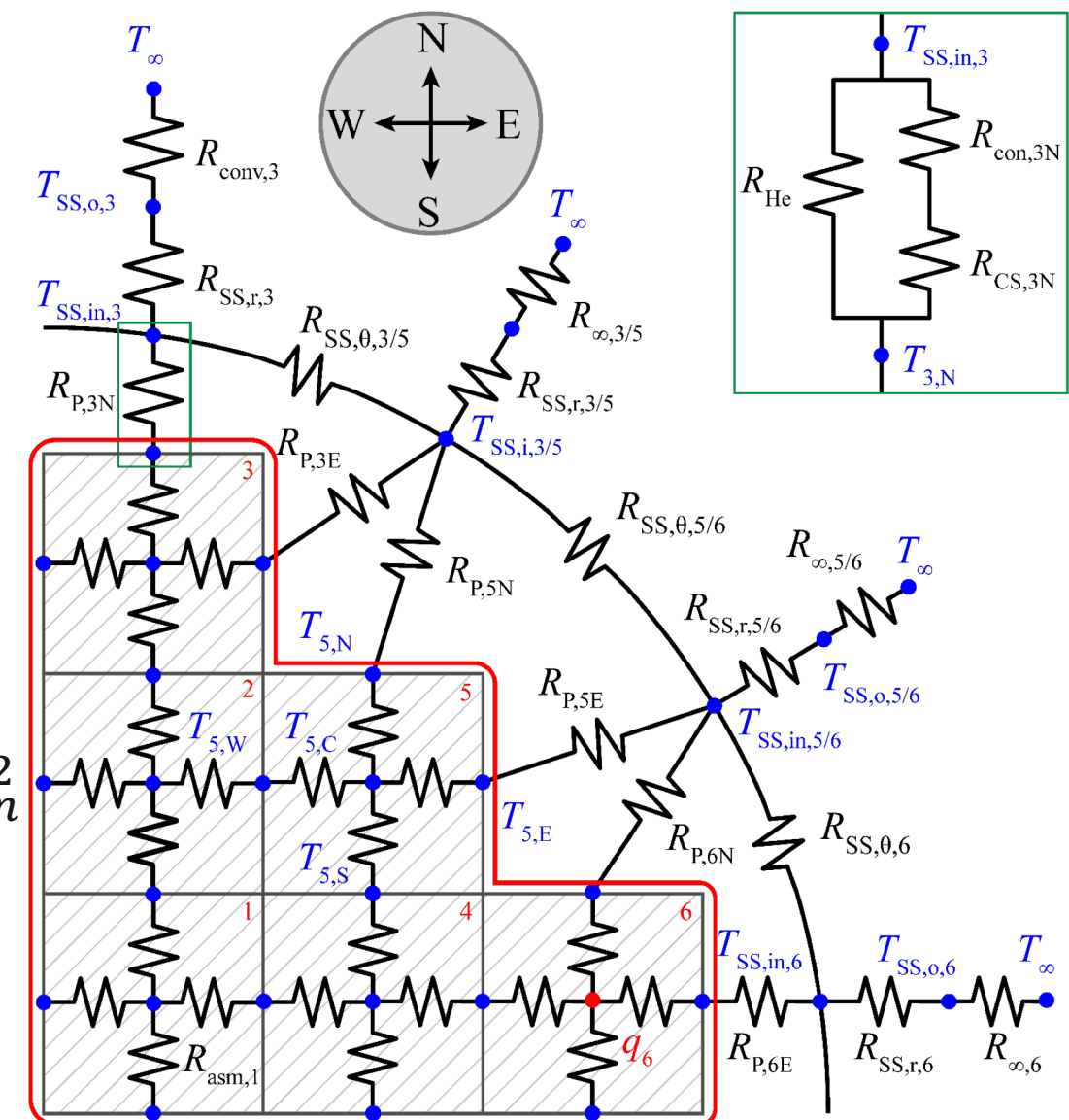
Conduction: Fuel Assemblies

Thermal resistance of assembly:

$$R_{asm} = \frac{R_o^2}{4\kappa_{eff} V_{asm}}$$

Effective thermal conductivity^[3]:

$$\begin{aligned} \kappa_{eff} &= 0.3940 + 1.334 \times 10^{-3} T_m + 2.849 \times 10^{-6} T_m^2 \\ &+ 8.359 \times 10^{-10} T_m^3 \end{aligned}$$



[3] R. BAHNEY and T. LOTZ, "Spent nuclear fuel effective thermal conductivity report," Prepared for the US DOE, Yucca Mountain Site Characterization Project Office by TRW Environmental Safety Systems, Inc., July 11(1996).



Conduction: Helium Back-fill and Spacers

Helium^[4]:

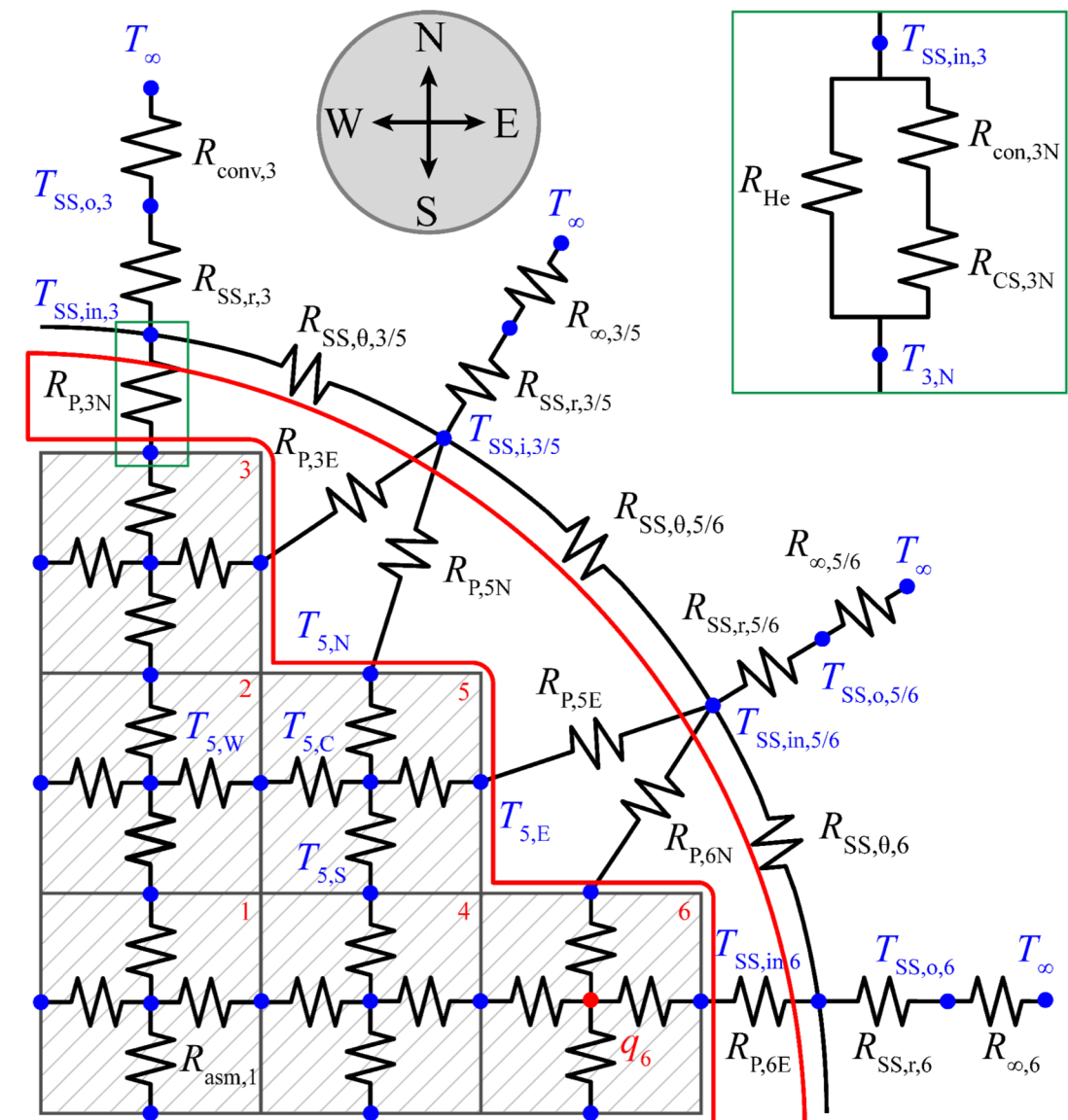
$$R_{He} = \frac{L_c}{\kappa_{He} A_c}$$

Carbon Steel:

$$R_{CS} = \frac{L_c}{\kappa_{CS} A_c} + R_{con,i}$$

Steel/Helium:

$$R_{eff} = \frac{R_{CS} R_{He}}{R_{CS} + R_{He}}$$



[4] V. D. ARP and R. D. MCCARTY, "Thermophysical Properties of Helium-4 from 0.8 to 1500 K with Pressures to 2000 MPa," Tech. rep., United States Department of Commerce, Technology Administration, National Institute of Standards and Technology (1989).

Conduction: Steel Canister

Stainless Steel:

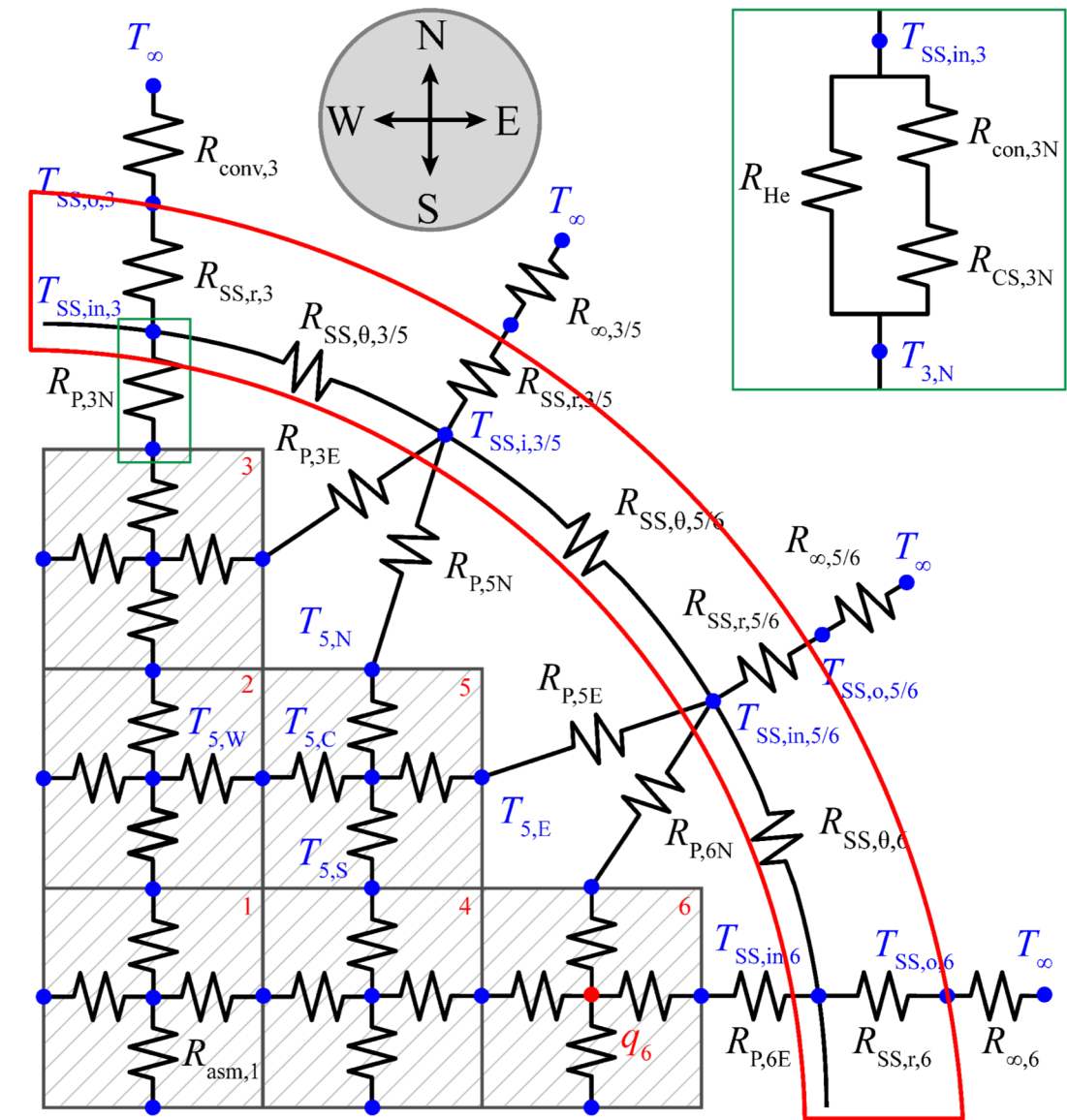
$$R_{SS,r} = \frac{\ln\left(\frac{r_o}{r_{in}}\right)}{2\pi L_{asm} k_{SS}}$$

Stainless Steel^a:

$$R_{SS,c} = \frac{\alpha}{k_{SS} A_{SS}}$$



^a α is the arc length between surface temperature nodes.



Convection: Canister Surface to Ambient

Convection:

$$R_{\infty} = \frac{1}{hA_c}$$

Convective heat transfer coefficient:

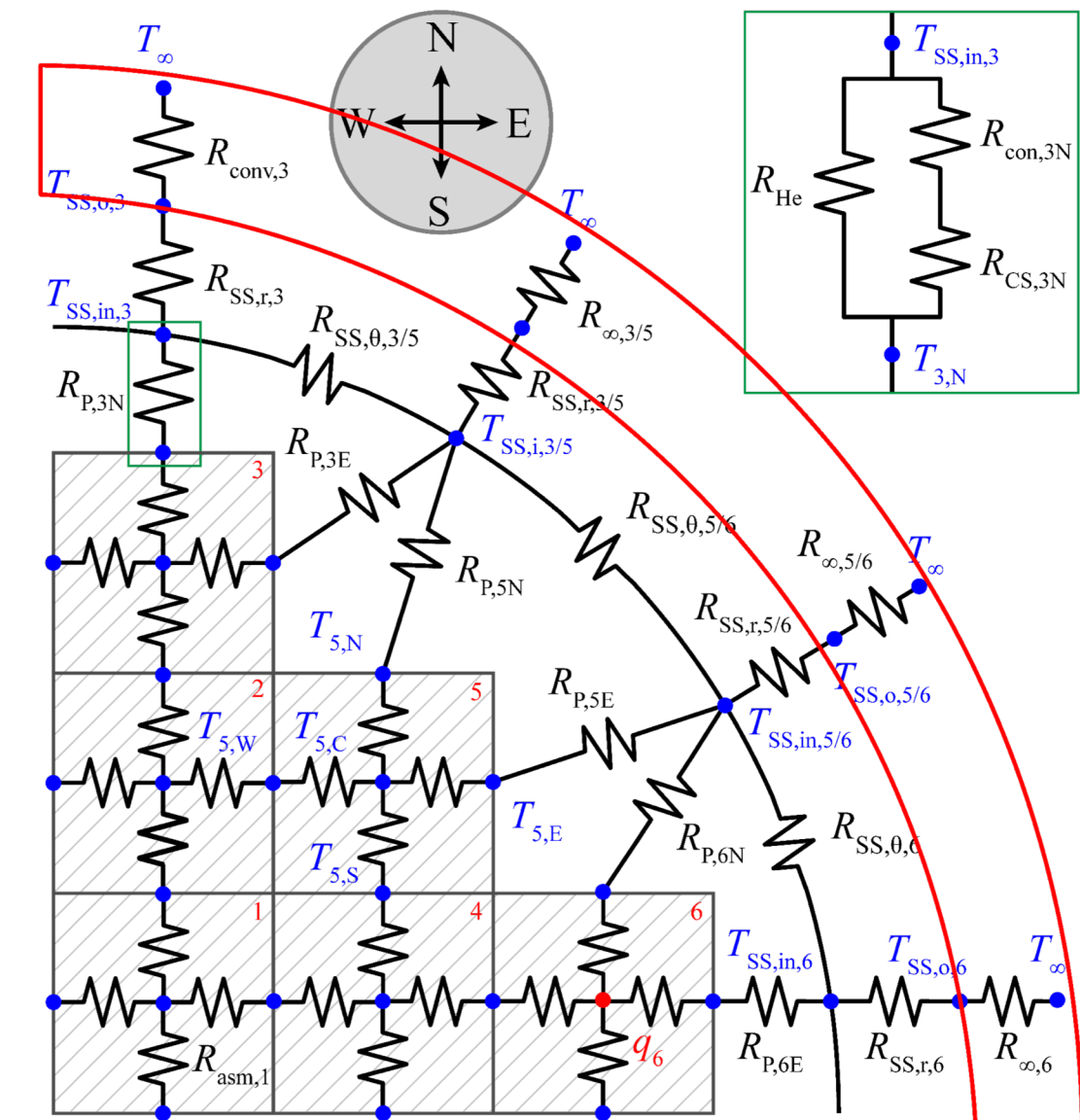
$$h = \frac{Nu_{eff} \kappa_{air}}{D}$$

Nusselt number:

$$Nu_{eff} = [Nu_D^3 + Nu_{local}^3]^{\frac{1}{3}}$$

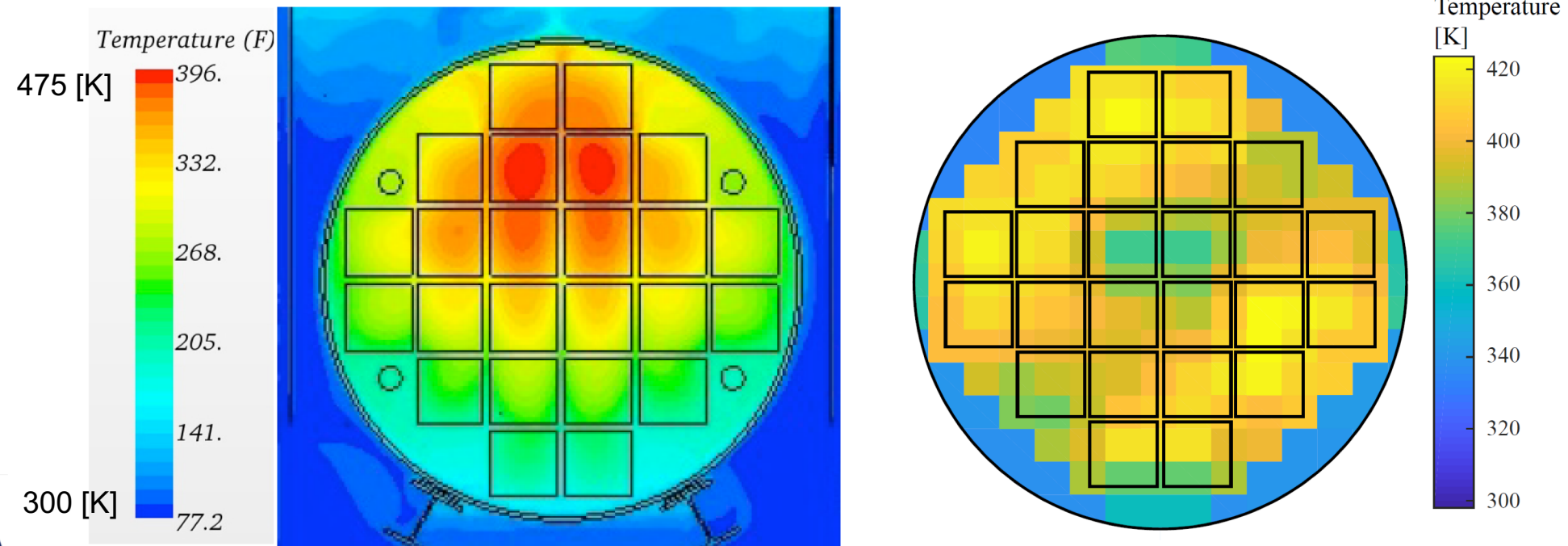
Nusselt number:

$$Nu_D = \begin{cases} 0.53 Ra_D^{0.25} & 10^4 \leq Ra_D \leq 10^9 \\ 0.13 Ra_D^{0.33} & Ra_D \geq 10^9 \end{cases}$$



Results and Comparison

Location	Measured [2]	Helium Free-Convection				Conduction-Only			
		[2]	% Diff.	TRN	% Diff.	[2]	% Diff.	TRN	% Diff.
North (90°)	321	345	9.8	-	-	346	7.5	335	4.3
East (0°)	315	331	5.0	-	-	336	6.5	332	5.4
Southeast (330°)	314	316	0.6	-	-	330	5.0	340	8.0
West (180°)	315	331	5.0	-	-	334	5.9	329	4.3
Southwest (270°)	315	316	0.3	-	-	329	4.3	338	7.0

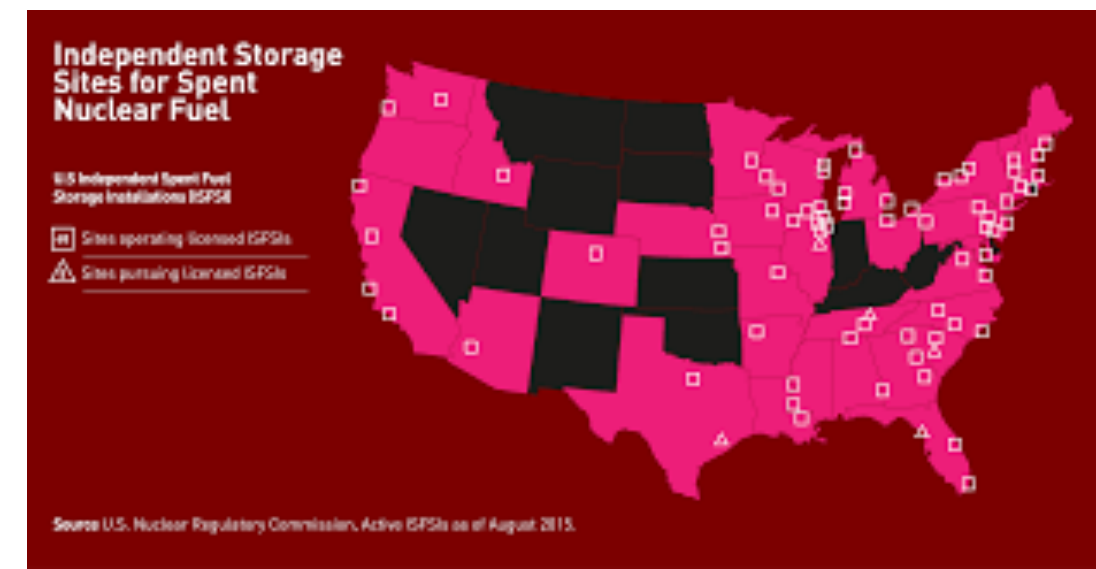
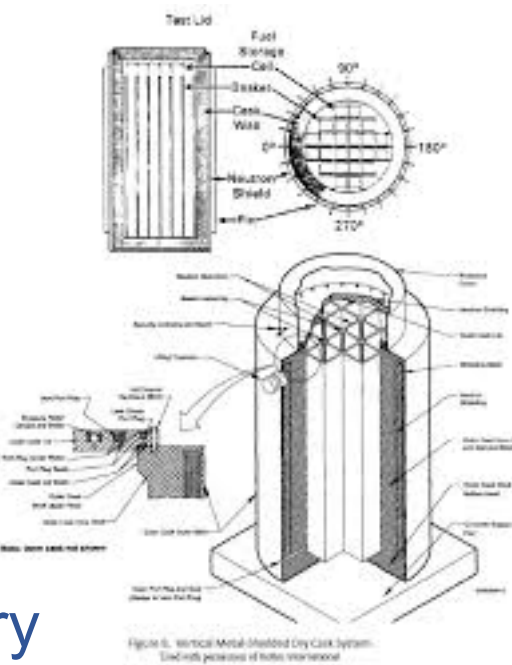


Temperature Distribution in Central Cross-section of HSM-15
for Summer Case – 77°F (25°C) Ambient^[2]



For the Future...

- Generalization
 - Fuel Decay
 - Variable Geometry



Supplementary Slides



Spacer Disc Contact Resistance^[2]

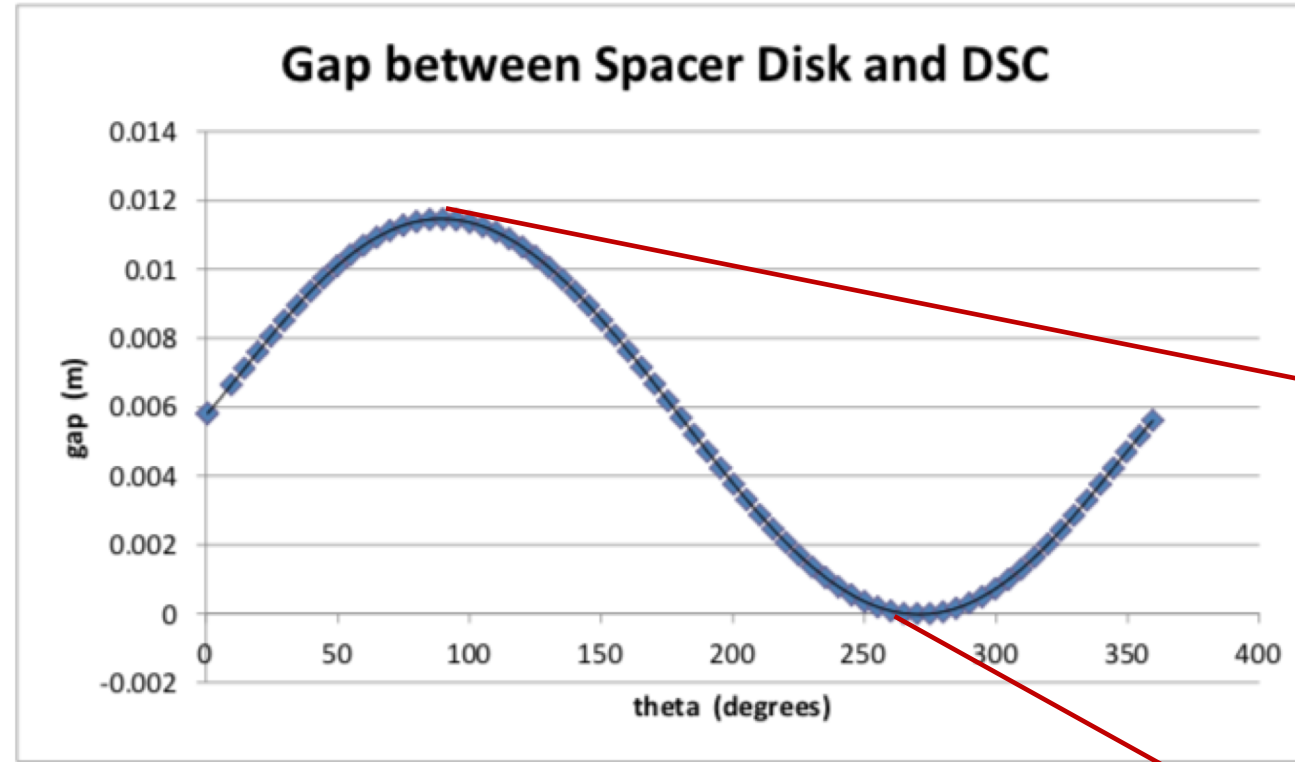


Figure C.1. Gap Between Spacer Disk and DSC in Relation to the Cylindrical Angle of the DSC

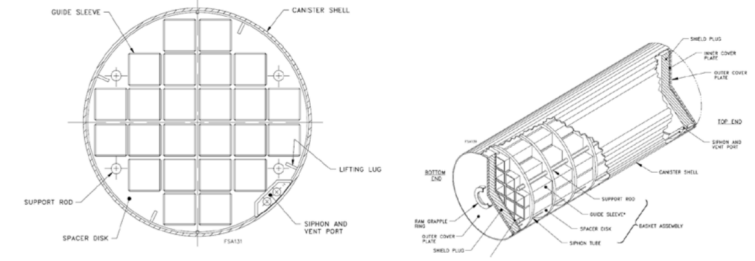


Figure 2.2. Illustrative Diagrams of 24P DSC Geometry (Images courtesy of AREVA)

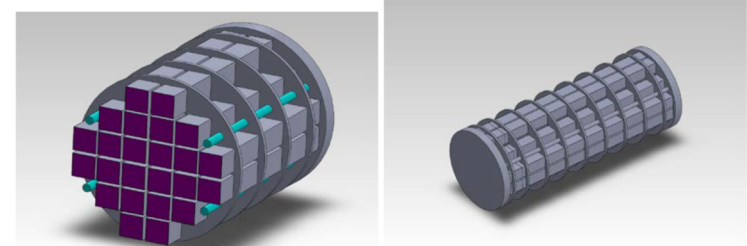
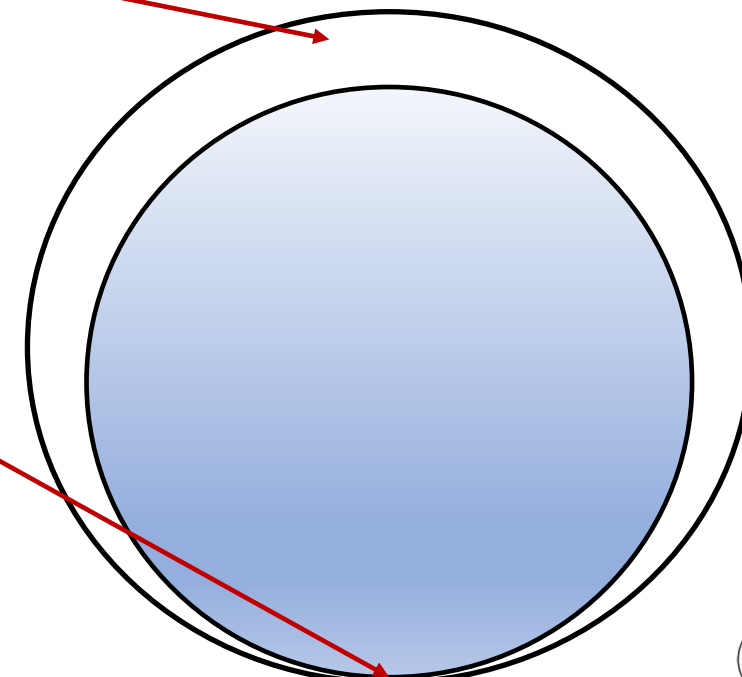


Figure 2.3. Mid-Plane Cross-Sectional View and Exterior View of Internal Geometry in SolidWorks® Model of 24P DSC



Fuel Decay Heat^[2]

Table 8.1. Fuel Assembly Decay Heat Loads for DSC in HSM-1 as of June 2012

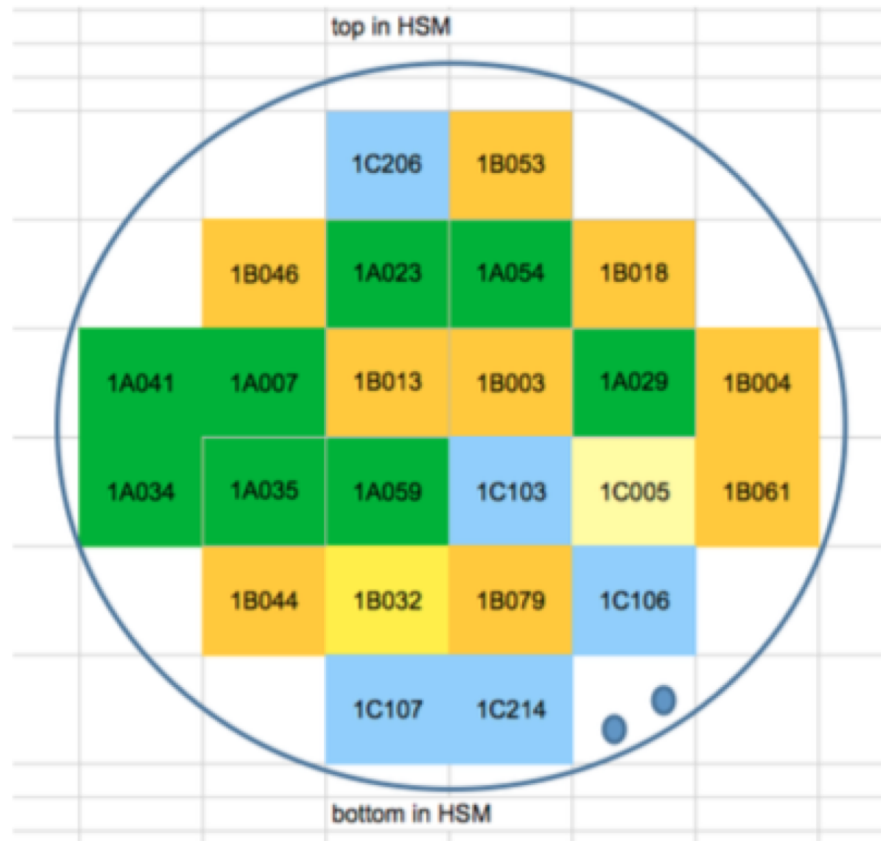


Figure 8.2. Fuel Assembly Loading and Identification Numbers for HSM-1



Fuel Assembly ID	Heat Load (kW)
1B013	0.1839
1B003	0.1989
1A007	0.1305
1A059	0.1374
1C103	0.1899
1A023	0.1375
1A054	0.1393
1B046	0.1922
1C005	0.1752
1B079	0.1874
1B032	0.1399
1A029	0.1382
1A035	0.133
1B004	0.1978
1B018	0.1977
1A034	0.1307
1C107	0.1894
1B053	0.1847
1B044	0.1955
1C206	0.2021

Fuel Decay Heat^[2]

Table 5.2. Fuel Assembly Decay Heat Loads for DSC in HSM-15 as of June 2012

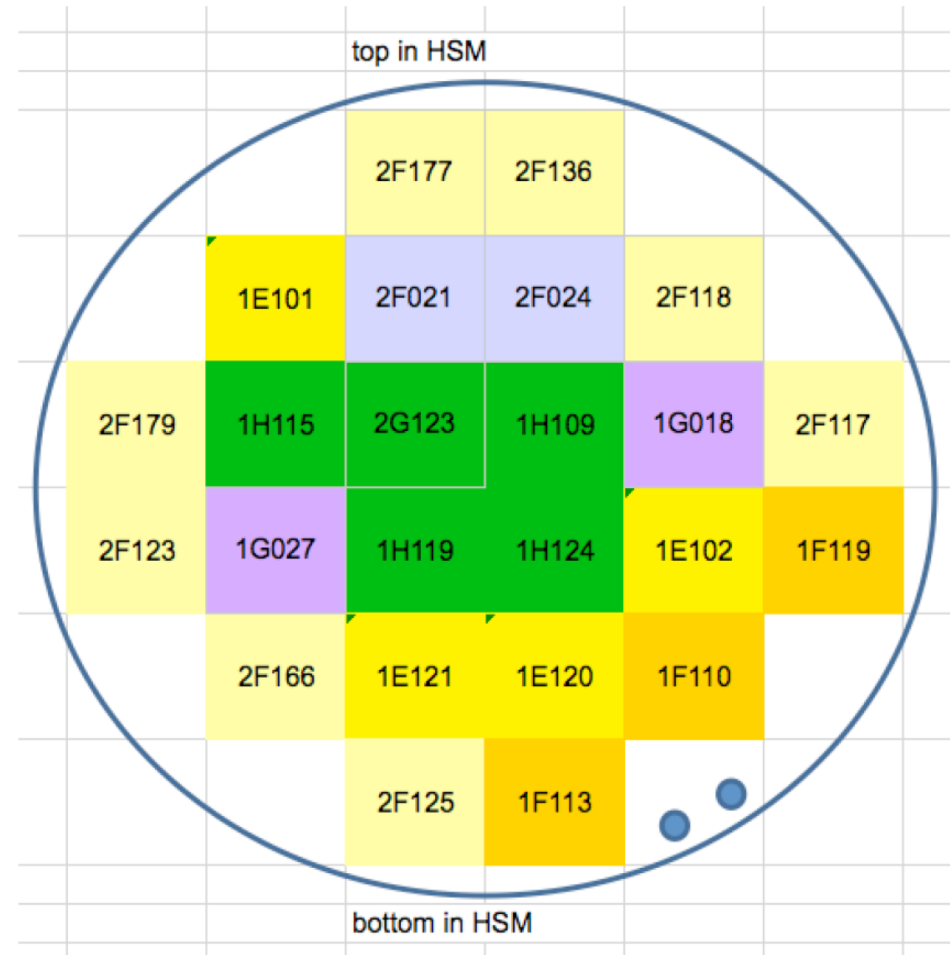


Figure 5.3. Fuel Assembly Loading and Identification Numbers

Fuel Assembly ID	Heat Load (kW)
2G123	0.427
1H109	0.407
1H115	0.406
1H119	0.408
1H124	0.407
2F021	0.385
2F024	0.385
1E101	0.301
1E102	0.301
1E120	0.302
1E121	0.302
1G018	0.327
1G027	0.340
2F117	0.285
2F118	0.286
2F123	0.285
2F125	0.274
2F136	0.291

